

New patterns in high-speed granular flows

Nicolas Brodu,^{1,2} Renaud Delannay,¹ Alexandre Valance,¹ and Patrick Richard^{1,3}

¹*Institut Physique de Rennes, UMR CNRS 6251,
Université de Rennes 1, Campus de Beaulieu Bâtiment 11A,
263 av. Général Leclerc, 35042 Rennes CEDEX, France*

²*Duke University, Dpt. of Physics, Box 90305, Durham NC 27708 USA*

³*LUNAM Université, IFSTTAR, GPEM, site de Nantes,
Route de Bouaye, 44344 Bouguenais cedex, France*

(Dated: March 28, 2014)

We report on new patterns in high-speed flows of granular materials obtained by means of extensive numerical simulations. These patterns emerge from the destabilization of unidirectional flows upon increase of mass holdup and inclination angle, and are characterized by complex internal structures including secondary flows, heterogeneous particle volume fraction, symmetry breaking and dynamically maintained order. Interestingly, despite their overall diversity, these regimes are shown to obey a universal scaling law for the mass flow rate as a function of the mass holdup. This unique set of 3D flow regimes raises new challenges for extending the scope of current granular rheological models and opens new perspectives for interpreting the features of geophysical granular flows.

PACS numbers:

Introduction– Granular gravity-driven flows are very common in industrial and geophysical processes. These flows are generally dense, run on a flat frictional base and are confined by lateral walls or levees (due to self-channeling). The scientific community has paid particular attention to these flows over the last thirty years [1]. However, their modeling is still an open issue. The complexity comes from grain/grain interactions that include both collisions and long lasting frictional contacts. Identifying regions of the flow where one type of interaction prevails over the other is part of the issue to be resolved.

One of the most studied configurations is the inclined plane geometry. Partly because it is a simple and good model for many common situations, but also because it may be seen as a rheological test with constant friction. Indeed, if sidewall friction is negligible, for steady and fully developed (SFD) flows, the tangential and normal forces on the base correspond exactly to the components of the flow weight. Their ratio, which is nothing but the apparent friction μ , is equal to the tangent of the angle of inclination. To date, experiments and simulations have focused mainly on flows with moderate inclination, leading to fairly simple unidirectional SFD flows [1]. However, more complex SFD flows with spanwise vortices were obtained for higher angles [2]. One therefore strongly expect that upon further increase of the inclination angle more and more complex flow features should emerge.

In the case of a flat frictional base, the ratio of the tangential to the normal component of the contact force acting on a grain in contact with the base has an upper bound which is the microscopic friction coefficient μ_m . Thereby, the effective friction $\mu = \tan \theta$ is also bounded by μ_m . For definite and realistic values of μ_m , this automatically limits the possible angles for SFD flows. In

the case of a bumpy base, the relation between μ_m and the limit for μ is more complex because of additional geometrical effects [1]. The easiest way to obtain SFD flows at high angles is to introduce frictional side walls. This is what we have done in the present work. If the grain/wall friction coefficient is high enough, one may expect that the base friction supplemented by the side wall friction will be able to balance the driving component of the weight.

We have conducted simulations of granular flows down flat and steep inclines with frictional side walls using a discrete element model (DEM). The principle of DEM simulations is to treat each grain as a sphere (of diameter D) subject to gravity and contact forces with both the other grains and the basal and lateral walls. These contact forces are characterized by a coefficient of restitution e , a coefficient of friction μ_m and a stiffness coefficient k (see Supplementary Table 1). The fundamental principle of dynamics is applied to calculate the motion of each individual particle. This method, which has successfully been used to simulate granular flows [3–5], has been optimized to obtain three-dimensional SFD flows within a reasonable computation time. We used periodic boundary conditions in the streamwise direction. The periodic cell had a length $L = 20D$ and width $W = 68D$. Simulations were run up to a stabilization of the total kinetic energy of the system. We obtained SFD flows for all the flow configurations we have investigated, varying extensively the inclination angle θ and the mass hold-up \tilde{H} (defined by $\tilde{H} = \int_0^\infty \phi(z) dz / D$ where ϕ is the particle volume fraction at height z).

Our simulations reveal the existence of unexpected SFD regimes which were never reported in the literature. These new regimes emerge from the destabilization of SFD unidirectional flows upon increase of the mass

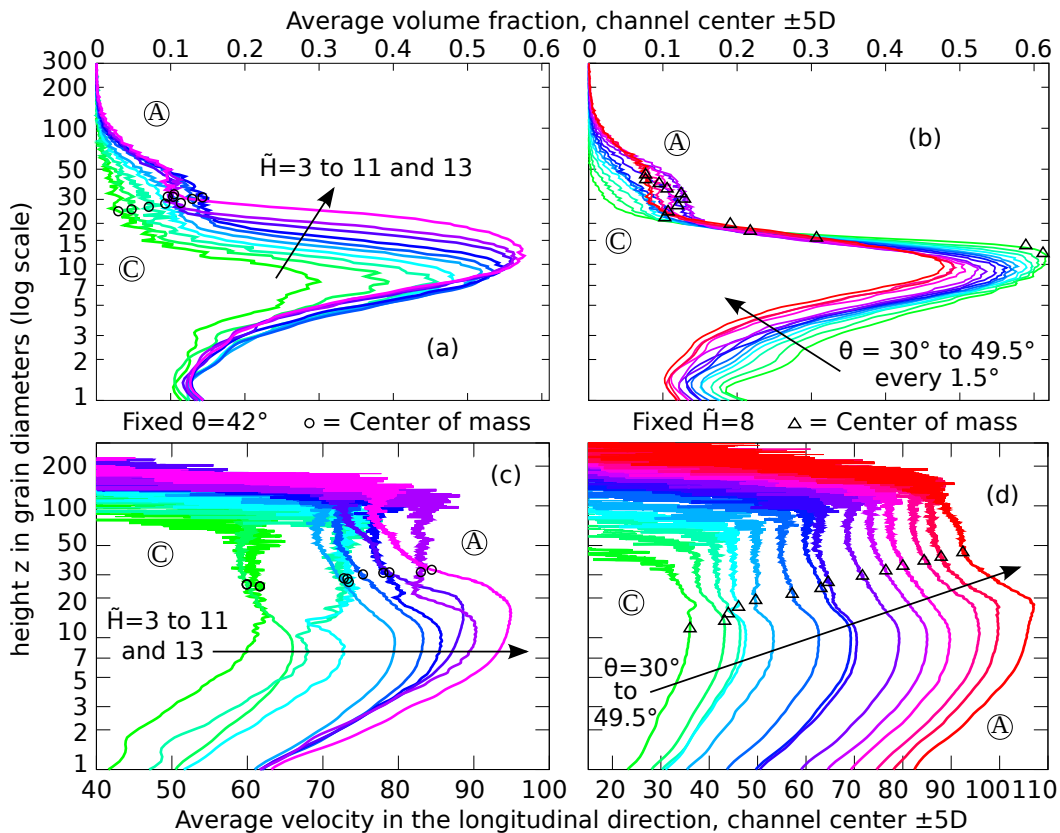


FIG. 1: Vertical profiles of the volume fraction of the flow ((a) and (b)) and of the velocity in the main flow direction ((c) and (d)). Both quantities are measured at the center of the channel and are averaged over $10D$ in the transverse direction. The curves reported in (b) and (d) are for a fixed mass holdup $\tilde{H} = 8$ and for different angles of inclination. Those reported in (a) and (c) are for a fixed angle of inclination $\theta = 42^\circ$ and for different values of mass holdup. Open circles and triangles indicate the vertical position of the center of mass which increases both with the mass holdup and the angle of inclination.

holdup and the slope. These flow regimes are likely to be encountered in many real situations and raise new challenges for extending the scope of current rheological models. We report below the various SFD flow regimes obtained upon variation of the slope and mass holdup and focus first on the supported flow regimes.

Supported regimes— Upon increase of the inclination angle, dense unidirectional flows destabilize and longitudinal rolls appear [2, 6, 7]. Upon further increase, a strongly sheared, dilute and agitated layer spontaneously appears at the base of the flow. Such a layer is able to support a dense packing of grains moving as a whole. These "supported" regimes have been already mentioned in the literature as a possible explanation for the unexpected high mobility of granular avalanches. Campbell [8] indeed suggested that the existence of a layer of highly agitated particles at low concentration beneath a densely packed main body could reduce the apparent basal friction and allow the flow to reach long runouts. Density inverted profiles are also predicted by the granular kinetic theory [9]. However, DEM simulations were unable up to

now to reproduce these flow regimes as steady and stable states. They were only observed as transient states in decelerated flows [8] or as a steady but unstable state at a unique value of the inclination angle [10]. In contrast, the "supported" regimes reported here are steady and fully developed, stable and were obtained within a large range of inclination angles.

Fig. 1 shows typical volume fraction and velocity profiles for SFD supported regimes. They present a dense core floating above a highly agitated granular gaseous phase, and topped by a dilute "atmosphere". The core is moving at a fast and almost uniform speed. The center of mass of the flow is located just on top of the core, so a large fraction of the matter is spread in the dilute atmosphere over a large distance. When the mass holdup increases the core lifts up and densifies (see Fig. 1a). Its lateral width decreases with increasing \tilde{H} because the lateral pressure pushes the grains toward the central core. This core can reach very high values of the volume fraction up to 0.6 at large mass holdup, while the volume fraction in the supporting basal gaseous layer is below 0.2. The existence of a stabilized dense core within a

very agitated and dilute region is probably a direct consequence of the clustering instability occurring in granular gas [11]. It is also worth noting that this flow regime bears a strong resemblance with that observed experimentally by Holyoake and McElwaine [12] on steep slopes with a "depletion layer" at the walls.

Above the dense core, the volume fraction is well described by a decreasing exponential: $\nu(z) \propto \exp(-z/H_C)$, where H_C represents the characteristic height of the atmosphere (see Supplementary Figure 1). The core slowly "evaporates" as the angle increases for a gradual transition to granular gas at larger angles (see Supplementary Figures 2 and 3). Surprisingly, when the angle θ increases, the altitude of the core remains constant (see Fig. 1b). However, the center of mass of the flow lifts up and the core thickness decreases as a non-negligible part of the material is transferred into the top granular gaseous phase. The vertical expansion of the flow is necessary to increase its friction on the lateral boundaries and to balance the driving force, which increases with the inclination angle. The basal friction cannot exceed $\mu_m Mg \cos \theta$, where $\mu_m = 0.59$ is the microscopic friction value used in the simulations [7] and M is the mass of the grains. Thus for large angles, a large part of the friction comes from the lateral walls as discussed in more details below.

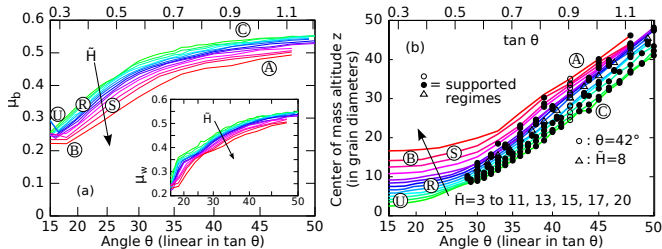


FIG. 2: (a) Effective friction coefficients on the base μ_b and the wall μ_w (inset) as a function of the inclination angle θ . Both coefficients increase with θ but show a reduction for increasing mass hold-up. (b) Altitude of the center of mass C_M as a function of θ for various mass hold-up. Markers indicate the states corresponding to the supported flow regimes for which C_M exhibits a linear increase with $\tan \theta$. Labels \textcircled{U} , \textcircled{R} , \textcircled{C} , \textcircled{A} , \textcircled{S} and \textcircled{B} refer to the different flow regimes defined in Fig. 3.

The effective friction coefficients respectively at the base μ_b and at the walls μ_w are computed as the ratio of tangential to normal stresses. Fig. 2a shows the dependency of μ_b and μ_w on θ and \tilde{H} . Both coefficients increase and saturate at high inclination angles. In contrast, they decrease with the mass holdup: for a given angle, the basal friction reduces as more matter is added in the flow. This reduction of basal friction with increasing mass hold-up has never been reported before and may be a clue for explaining the long run-out for large rock avalanches [8].

As mentioned earlier, the vertical extent of the flow is a key feature to understand the balance between the gravitational driving force and friction. The position C_M of the center of mass of the flow is a simple and interesting indicator which is shown in Fig. 2b. For the supported flows (indicated by dots in the Figure), C_M increases linearly with $\tan \theta$: $C_M = a \tan \theta + b$, where the slope $a = 54.6D$ is independent of the mass holdup. Using a simple force balance, it can be shown that the slope is simply given by $a \approx W/2\mu_m$ (see Supplementary Note 1). In contrast, the parameter b increases with mass holdup and reflects the corresponding increase of the core thickness with \tilde{H} described in Fig. 1a.

Phase Diagram– In addition to the supported flows, we have discovered a myriad of new regimes by exploring extensively and systematically the parameter space (θ, \tilde{H}) . We report in Fig. 3 the domain of existence of the different identified regimes. These are labeled by circled letters and are briefly described below:

- Regime \textcircled{U} corresponds to classical Unidirectional dense flows.
- Regime \textcircled{R} corresponds to flows with Rolls previously reported in experimental and numerical works [2, 6, 7].
- Regime \textcircled{C} stands for the supported regime described previously.
- Regime \textcircled{A} denotes the supported regime with asymmetric core. As the mass holdup increases, the initial axisymmetric dense core starts to swing back and forth from left to right and loses its axial symmetry. For larger \tilde{H} and θ , a "plume" eventually forms on top of the core, as shown in the snapshots of Fig. 3.
- Regime \textcircled{S} corresponds to the Superposed rolls and appears at larger mass holdups \tilde{H} than regime \textcircled{R} . An example is shown in the snapshots of Fig. 3.

– Regime \textcircled{B} is characterized by the presence of a Basal layered structure. The observed order (see snapshots of Fig. 3) is dynamically maintained by collisions and cage effects. The layers are sheared and not static. Rolls are present in the disordered zone on the top of the basal layers and are localized close to the lateral walls.

These different flow regimes open many perspectives to test the relevance of granular rheological models. For example, our results may be interpreted in the framework of the second-order fluid model proposed in [13] which predicts that shallow flows develop curved surface, as seen for regimes \textcircled{B} and \textcircled{C} .

Universal behavior– Although these flow regimes exhibit marked difference in terms of structural organization, they surprisingly show common features. First, the transient regime necessary to reach the steady state is well described by a simple exponential saturation for any value of the inclination angle and mass hold-up: $V(t) = V_L - (V_L - V_0) \exp(-t/\tau)$, where $V(t)$ is the average streamwise flow velocity at time t , V_0 the initial

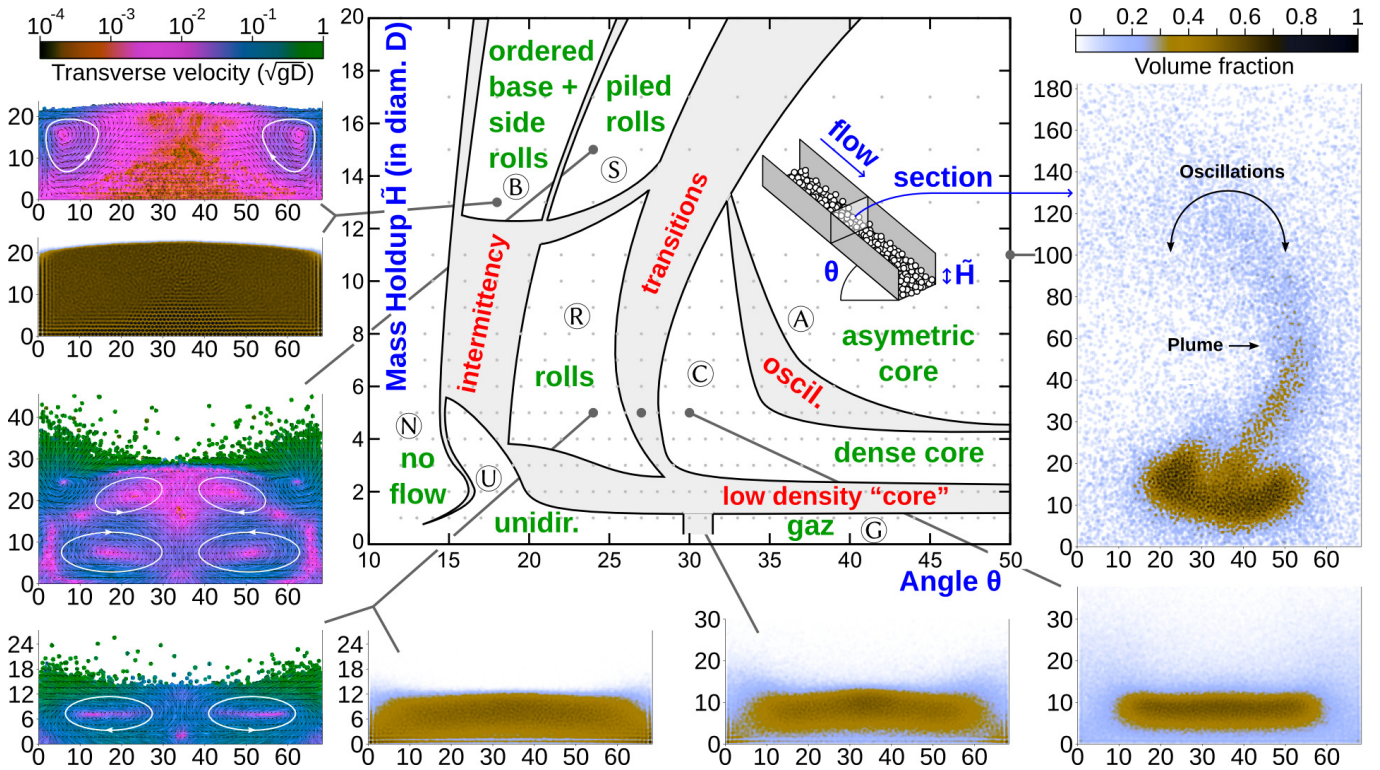


FIG. 3: Phase diagram in the *mass holdup* - *angle of inclination* space. (U): Unidirectional flows; (R): flows with Rolls; (C): flows with dense Core (i.e., supported flows); (A): supported flows with Asymmetric core; (S): flows with Superposed rolls; (B): flows with a Basal ordered layer topped by rolls. The 385 gray dots are the sampling points in the phase space where we performed a simulation. The phase diagram is supplemented with 2D maps representing the velocity in the transverse direction (left panels) and the particle volume fraction (middle and right panels).

flow velocity, and V_L the limit velocity (see Fig. 4a). The characteristic time τ is an increasing function of the mass hold-up and has a non-monotonic variation with the inclination angle (see Supplementary Figure 4a). This exponential velocity saturation suggests that the flow surprisingly experiences a viscous-like drag force proportional to the velocity (see Supplementary Figure 4b).

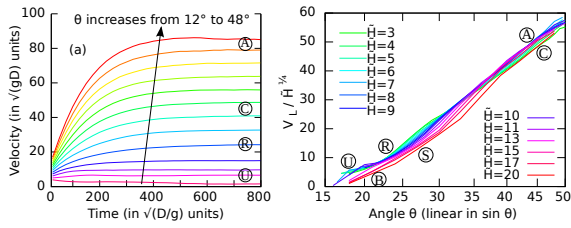


FIG. 4: (a) Typical temporal evolution of the mean flow velocity, for $\tilde{H} = 5$ and $\theta = 12^\circ$ to $\theta = 48^\circ$ every 3° . All the flows reach a steady state via an exponential saturation. (b) Rescaled steady state velocity $V_L/\tilde{H}^{1/4}$ as a function of $\sin \theta$ for various mass hold-up. The collapse is remarkable given the wide diversity of regimes. The scaling law simply reads: $V_L/\tilde{H}^{1/4} \approx A \sin \theta + B$, with $A \approx 122$ and $B \approx -37$.

Second, we identify a simple universal dependency of

the limit velocity on the mass hold-up and inclination angle: $V_L/\tilde{H}^{1/4} \approx A \sin \theta + B$, where A and B are constant coefficients. Figure 4b, reports the limit velocity V_L rescaled by $\tilde{H}^{1/4}$ versus the inclination angle θ for various mass holdups. A remarkable collapse is observed, given the large diversity of the flow regimes. In steady state, the mass flow rate is simply given by $Q = V_L \tilde{H}$ such that $Q \propto \tilde{H}^{5/4}$, which is close to the scaling law ($Q \propto \tilde{H}^{3/2}$) obtained experimentally over a smaller range of flow rate Q [14].

Conclusion— Using a simple flow configuration with flat lateral and basal boundaries, we have discovered, by increasing the inclination angle and mass holdup, new steady and fully developed regimes which present non-trivial features including heterogeneous volume fraction, secondary flows, symmetry breaking and dynamically maintained order. Despite the diversity of the features of these states, we have highlighted that the mass flow rate obeys a universal scaling law in terms of \tilde{H} . Explaining these regularities is a challenging issue as they suggest a unified underlying model.

A crucial question is to which extent these regimes and their features are specific to the material parameters and the confined geometry we have considered. Additional

simulations, where we have varied the material parameters (friction and restitution coefficient) and the basal conditions (flat or bumpy), lead to similar regimes as long as grain/wall friction prevails on grain/grain friction. Side walls play of course an important role regarding the friction and allow SFD flows for any value of the chute inclination. Without side walls, flows at large angle would not be steady but accelerated. Despite of this, analog flow regimes appear but as transient state (see Fig. S5). Furthermore, we are also convinced that the confined geometry may be relevant to granular geophysical flows, which are often either confined by the topography [15, 16] or self-channelized by the formation of levees [17, 18].

These results provide a unique set of granular flow regimes for testing theoretical and rheological models, and should also encourage investigations of granular flows for wider channels and higher mass holdup.

Acknowledgments— This work was partly financed by the RISC-E RTR and Région Bretagne (CREATE Sampleo grant). We thank Michel Louge, Jim McElwaine, Anne Mangeney and Olivier Roche for helpful discussions and comments on our work.

[1] GDR-MiDi, Eur. Phys. J. E **14**, 341 (2004).

[2] T. Börzsönyi, R. E. Ecke, and J. N. McElwaine, Phys. Rev. Lett. **103**, 178302 (2009).

[3] P. Cundall and O. Strack, Géotechnique **29**, 47 (1979).

[4] L. E. Silbert, D. Ertas, G. S. Grest, T. C. Halsey, D. Levine, and S. J. Plimpton, Phys. Rev. E **64**, 051302 (2001).

[5] S. Luding, Eur. J. Env. Civil Eng. **12**, 785 (2008).

[6] Y. Forterre and O. Pouliquen, J. Fluid Mech. **467**, 361 (2002).

[7] N. Brodu, P. Richard, and R. Delannay, Phys. Rev. E **87**, 022202 (2012).

[8] C. S. Campbell, The Journal of Geology **97**, 653 (1989).

[9] J. T. Jenkins and E. Askari, Chaos **9**, 654 (1999).

[10] N. Taberlet, P. Richard, J. T. Jenkins, and R. Delannay, Euro. Phys. J. E: Soft Mat. Bio. Phys. **22** (2007).

[11] S. McNamara and W. R. Young, Phys. Rev. E. **50**, 28 (1994).

[12] A. J. Holyoake and J. N. McElwaine, Journal of Fluid Mechanics **710**, pp 35 (2012).

[13] J. McElwaine, D. Takagi, and H. Huppert, Granular Matter **14**, 229 (2012).

[14] M. Y. Louge and S. C. Keast, Phys. Fluids **13**(5), 1213 (2001).

[15] G. Lube, S. J. Cronin, T. Platz, A. Freundt, J. N. Procter, C. Henderson, and M. F. Sheridan, Journal of Volcanology and Geothermal Research **161**, 165 (2007).

[16] P. Favreau, A. Mangeney, A. Lucas, G. Crosta, and F. Bouchut, Geophysical Research Letters **37**, L15305 (2010).

[17] N. Mangold, A. Mangeney, V. Migeon, V. Ansan, A. Lucas, D. Baratoux, and F. Bouchut, J. Geophys. Res. **115**, E11001 (2010).

[18] D. Jessop, K. Kelfoun, P. Labazuy, A. Mangeney, O. Roche, J.-L. Tillier, M. Trouillet, and G. Thibault, Journal of Volcanology and Geothermal Research **245-246**, 81 (2012).